Selective formic acid dehydrogenation catalyzed by Fe-PNP pincer complexes based on the 2,6-diaminopyridine scaffold

Irene Mellone,[a] Nikolaus Gorgas,[b] Federica Bertini,[a] Maurizio Peruzzini,[a] Karl Kirchner,*[,b] and Luca Gonsalvi*[,a]

[a] Consiglio Nazionale delle Ricerche (CNR), Istituto di Chimica dei Composti Organometallici (ICCOM), Via Madonna del Piano 10, 50019 Sesto Fiorentino (Firenze), Italy. Email: l.gonsalvi@iccom.cnr.it

[b] Institute of Applied Synthetic Chemistry, Vienna University of Technology, Getreidemarkt 9/163-AC, A-1060 Wien, Austria. Email: karl.kirchner@tuwien.ac.at

SUPPORTING INFORMATION

1. ADDITIONAL TABLES AND REACTION PROFILES

Table S1. Effect of the FA/NEt_3 ratio on the catalytic activity of **2**.[a]

Entry	NEt_3 (mol%)	TOF_{1h}[b]	TON[c]	conversion (%)
1	25	102	204 (3)	20
2	50	276	653 (3)	65
3	100	398	816 (3)	82
4	200	418	827 (3)	83

[a] Reaction conditions: **2** (0.01 mmol); FA (10 mmol); specified amount of NEt_3, THF (4.0 mL), 60 °C. Gas evolution measured by manual gas buret. [b] Defined as $mmol_{H2\ produced}$ / $mmol_{catalyst}$ x h^{-1} (calculated after 1h). [c] Defined as $mmol_{H2\ produced}$ / $mmol_{catalyst}$. Run time (h) in parenthesis. All tests were repeated at least twice to check for reproducibility (error ± 10%).

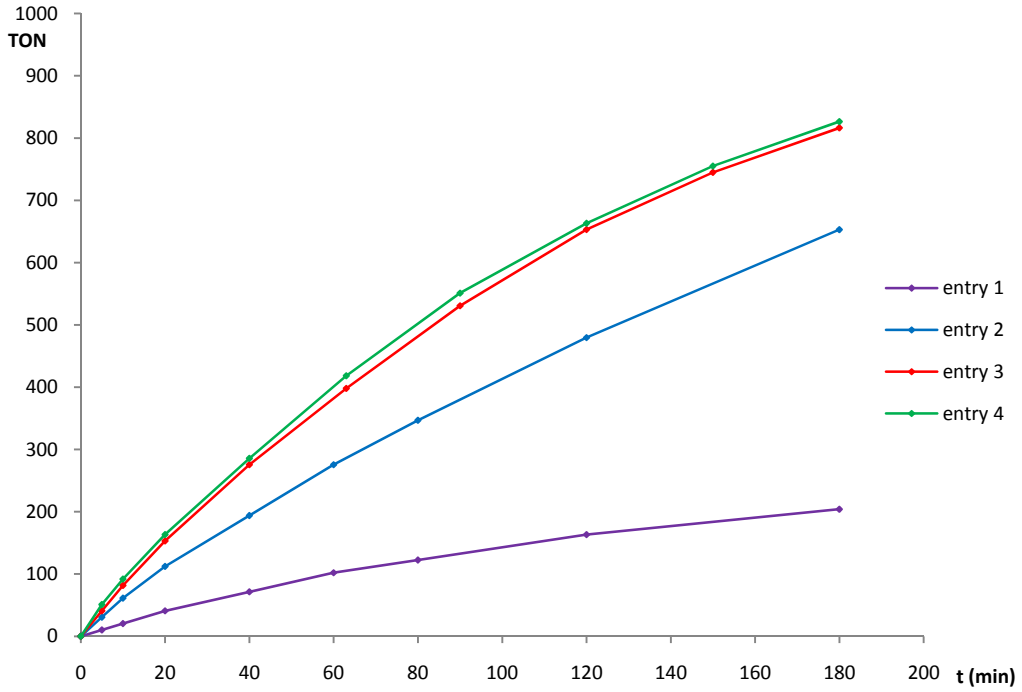

Figure S1. Reaction profiles for FA/NEt_3 ratio effect screening in FA dehydrogenation with **2**.

Table S2. Effect of different solvents on the catalytic activity of **2**.[a]

Entry	solvent	TOF_{1h}[b]	TON[c]	conversion (%)
1	THF	612	1000 (3)	100
2	PC	500	1000 (3)	100
3	dioxane	378	878 (3)	88
4	EtOH	165	650 (3)	65

[a] Reaction conditions: **2** (0.01 mmol); FA (10 mmol); NEt_3 (100 mol%), solvent (2.0 mL), 60 °C. Gas evolution measured by manual gas buret. [b] Defined as $mmol_{H2\ produced}$ / $mmol_{catalyst}$ x h^{-1} (calculated after 1h). [c] Defined as $mmol_{H2\ produced}$ / $mmol_{catalyst}$. Run time (h) in parenthesis. All tests were repeated at least twice to check for reproducibility (error ± 10%).

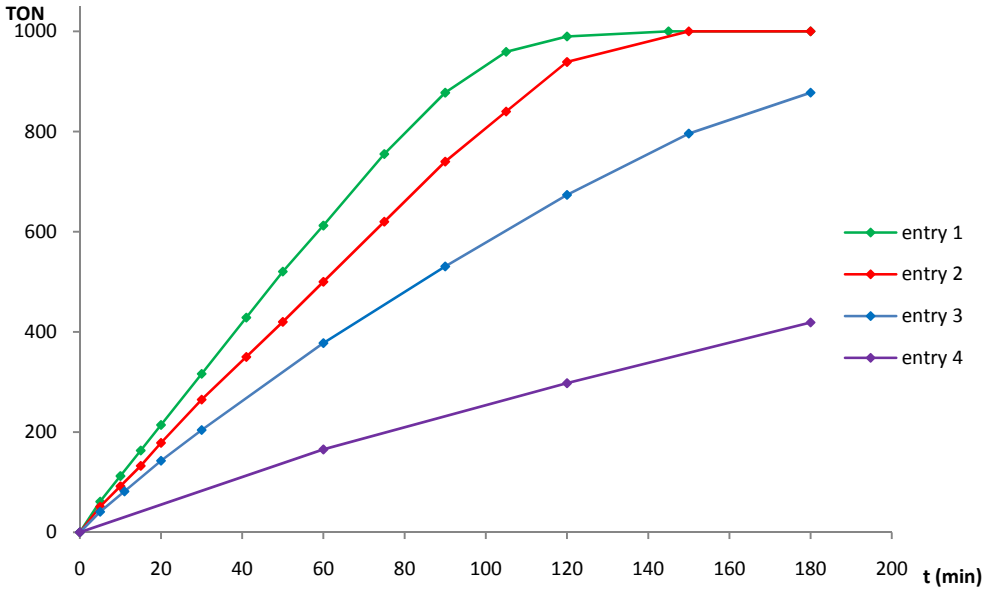

Figure S2. Reaction profiles for solvent effect screening in FA dehydrogenation with **2**.

Table S3. Effect of different amines on the catalytic activity of **2**.[a]

Entry	amine (mol%)	TOF_{1h}[b]	TON[c]	conv. (%)
1	NEt_3 (50)	593	980 (3)	98
2	DMOA (50)	673	980 (3)	98
3	DBU (50)	459	571 (3)	57

[a] Reaction conditions: **2** (0.01 mmol); FA (10 mmol); specified amine (50 mol%), THF (2.0 mL), 60 °C. Gas evolution measured by manual gas buret. [b] Defined as $mmol_{H2\ produced}$ / $mmol_{catalyst}$ x h^{-1} (calculated after 1h). [c] Defined as $mmol_{H2\ produced}$ / $mmol_{catalyst}$. Run time (h) in parenthesis. All tests were repeated at least twice to check for reproducibility (error ± 10%).

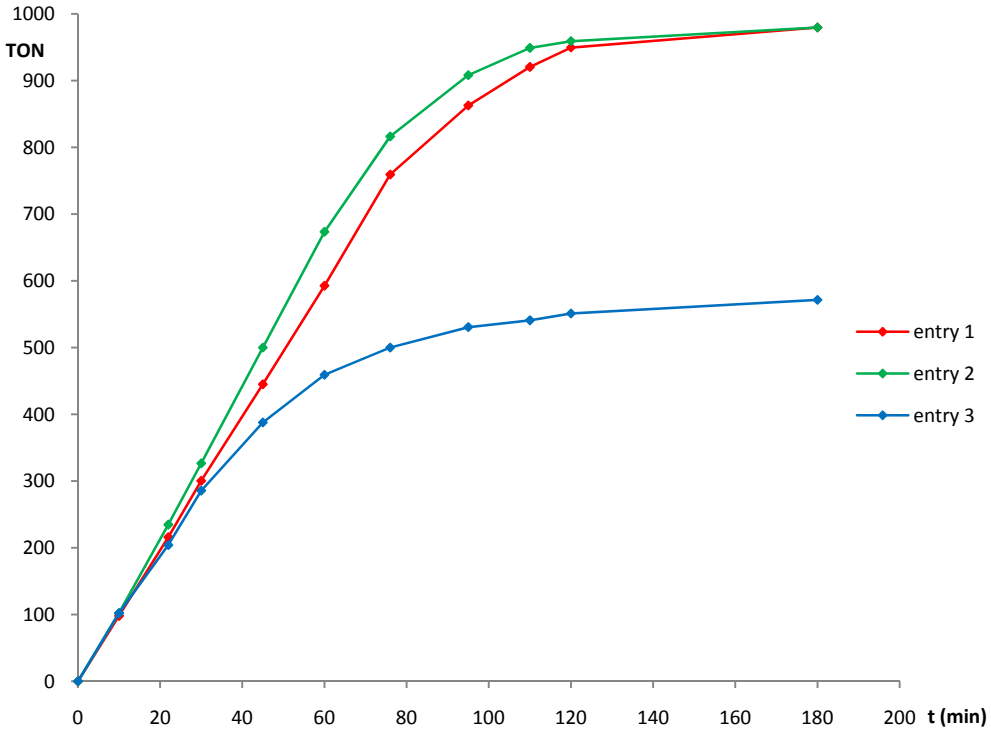

Figure S3. Reaction profiles for amine effect screening in FA dehydrogenation with **2**.

Table S4. Effect of the reaction temperature on the catalytic activity of **2**.

Entry	Solvent	T (°C)	TOF_{1h} [b]	TON[c]	conv. (%)
1	THF	40	79	180 (3)	18
2	THF	60	612	1000 (3)	100
3	PC	60	500	1000 (3)	100
4	PC	80	1800 [d]	1000 (0.6)	100

[a] Reaction conditions: **2** (0.01 mmol); FA (10 mmol); NEt_3 (100 mol%), solvent (2.0 mL). Gas evolution measured by manual gas buret. [b] Defined as $mmol_{H2\ produced}$ / $mmol_{catalyst}$ x h^{-1} (calculated after 1h). [c] Defined as $mmol_{H2\ produced}$ / $mmol_{catalyst}$. Run time (h) in parenthesis. [d] TOF calculated after 20 min due to fast reaction. All tests were repeated at least twice to check for reproducibility (error ± 10%).

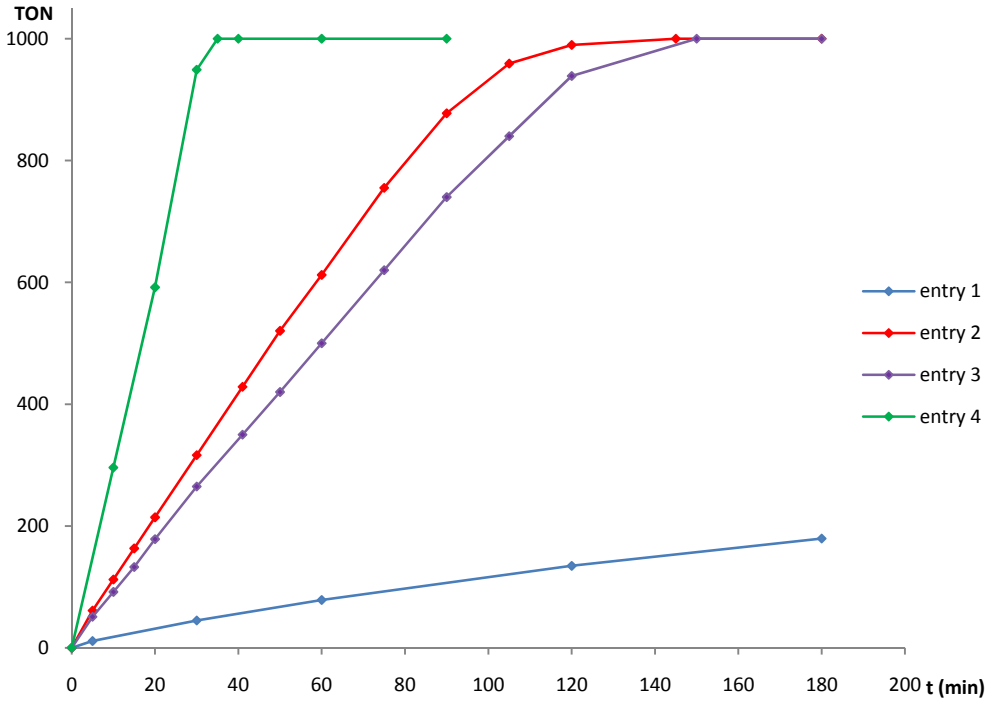

Figure S4. Reaction profiles for temperature effect screening in FA dehydrogenation with **2**.

Table S5. Effect of the substrate concentration on the catalytic activity of **2**.

Entry	[FA] (mol/L)	TOF_{1h}[d]	TON[e]	conversion (%)
1[a]	2.5	398	816 (3)	82
2[b]	5.0	612	1000 (2.5)	100
3[c]	10.0	770	1000 (2)	100

Reaction conditions: [a] **2** (0.01 mmol); FA (10 mmol); NEt_3 (100 mol%), THF (4.0 mL), 60°C. [b] THF (2.0 mL). [c] THF (1.0 mL). Gas evolution measured by manual gas buret. [d] Defined as $mmol_{H2\ produced}$ / $mmol_{catalyst}$ x h^{-1} (calculated after 1h). [e] Defined as $mmol_{H2\ produced}$ / $mmol_{catalyst}$. Run time (h) in parenthesis. All tests were repeated at least twice to check for reproducibility (error ± 10%).

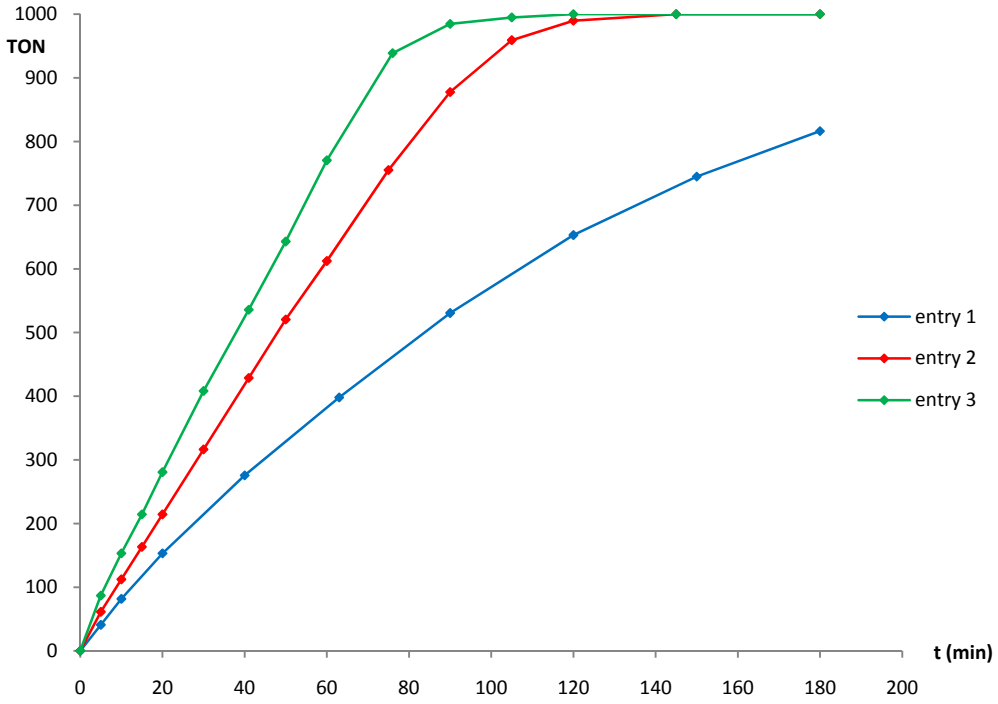

Figure S5. Reaction profiles for substrate concentration effect screening in FA dehydrogenation with **2**.

Table S6. Effect of catalyst loading on the catalytic activity of **2**.

Entry	[FA](mol/L)	solvent	T (°C)	TOF_{1h}[d]	TON[e]	conversion (%)
1[a]	10.0	THF	60	918	2245 (6)	22
2[b]	5.0	PC	80	1714	6286 (6)	63
3[c]	10.0	PC	80	2635	10000 (6)	100

Reaction conditions: [a] **2** (0.005 mmol); FA (50 mmol); NEt_3 (100 mol%), THF (5.0 mL), 60 °C. [b] **2** (0.005 mmol); FA (50 mmol); NEt_3 (100 mol%), PC (10.0 mL), 80 °C. [c] **2** (0.005 mmol); FA (50 mmol); NEt_3 (100 mol%), PC (5.0 mL), 80 °C. Gas evolution measured by manual gas buret. [d] Defined as $mmol_{H2\ produced}$ / $mmol_{catalyst}$ x h^{-1} (calculated after 1h). [e] Defined as $mmol_{H2\ produced}$ / $mmol_{catalyst}$. Run time (h) in parenthesis. All tests were repeated at least twice to check for reproducibility (error ± 10%).

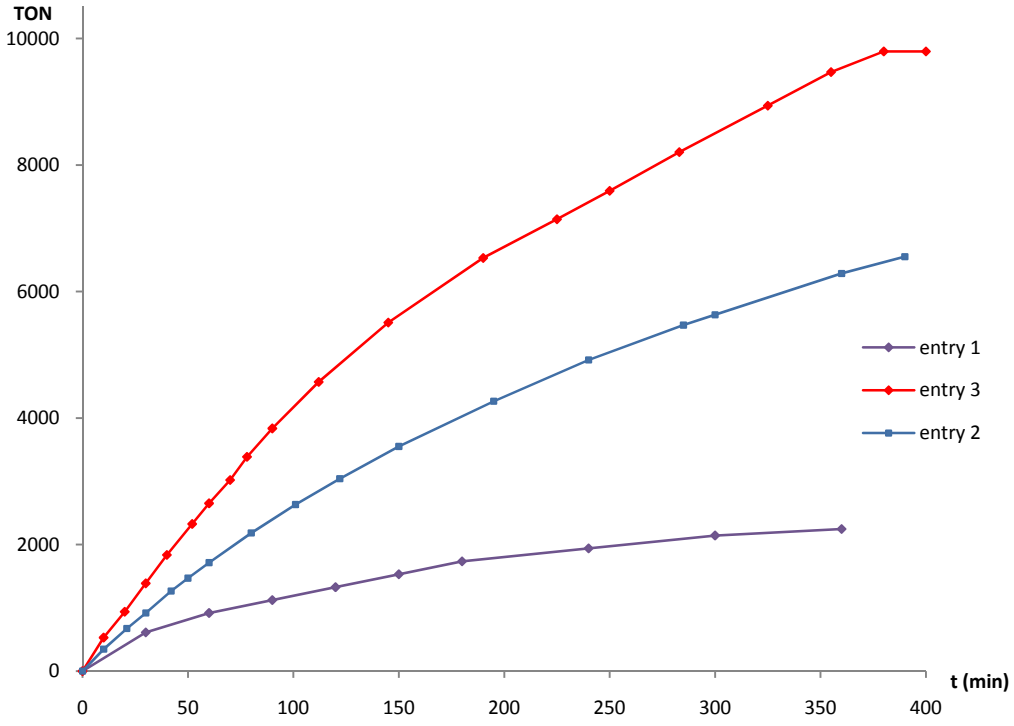

Figure S6. Reaction profiles for catalyst loading effect screening in FA dehydrogenation with **2**.

Table S7. Slow FA addition tests in the presence of **2** and **3** and NEt_3.

Entry	No. run	Initial FA/cat	$TOF_{10\ min}$[d]	TON[e]	conversion (%)[f]
1[a]	1	5000	2574	2500	50 (65)
	2		2628	2500	50 (135)
	3		2439	2500	50 (230)
	4		2140	2500	50 (350)
	5		1874	2170	47 (520)
2[b]	1	1000	1782	502	50 (17)
	2		1715	502	50 (35)
	3		1668	502	50 (52)
	4		1795	502	50 (70)
	5		1727	502	50 (87)
	6		1701	502	50 (105)
	7		1724	502	50 (122)
	8		1710	502	50 (145)
	9		1616	502	50 (175)
	10		1517	502	50 (210)
	11		1401	502	50 (250)
	12		1279	52	5 (270)
3[c]	1	5000	2844	2500	50 (60)
	2		2664	2500	50 (130)
	3		2494	2500	50 (225)
	4		2141	2500	50 (345)
	5		1882	2300	48 (550)

Reaction conditions: [a] **2** (0.005 mmol); FA (25 mmol, initial); NEt_3 (100 mol%), PC (5.0 mL), 80 °C. [b] **2** (0.01 mmol); FA (10 mmol, initial); NEt_3 (100 mol%), PC (5.0 mL), 80 °C. : [c] **3** (0.005 mmol); FA (25 mmol, initial); NEt_3 (100 mol%), PC (5.0 mL), 80 °C. [d] Defined as $mmol_{H2\ produced}$ / $mmol_{catalyst}$ x h^{-1} (calculated after 10 min). [e] Defined as $mmol_{H2\ produced}$ / $mmol_{catalyst}$. [f] Run time (min) in parenthesis. All tests were repeated at least twice to check for reproducibility (error ± 10%).

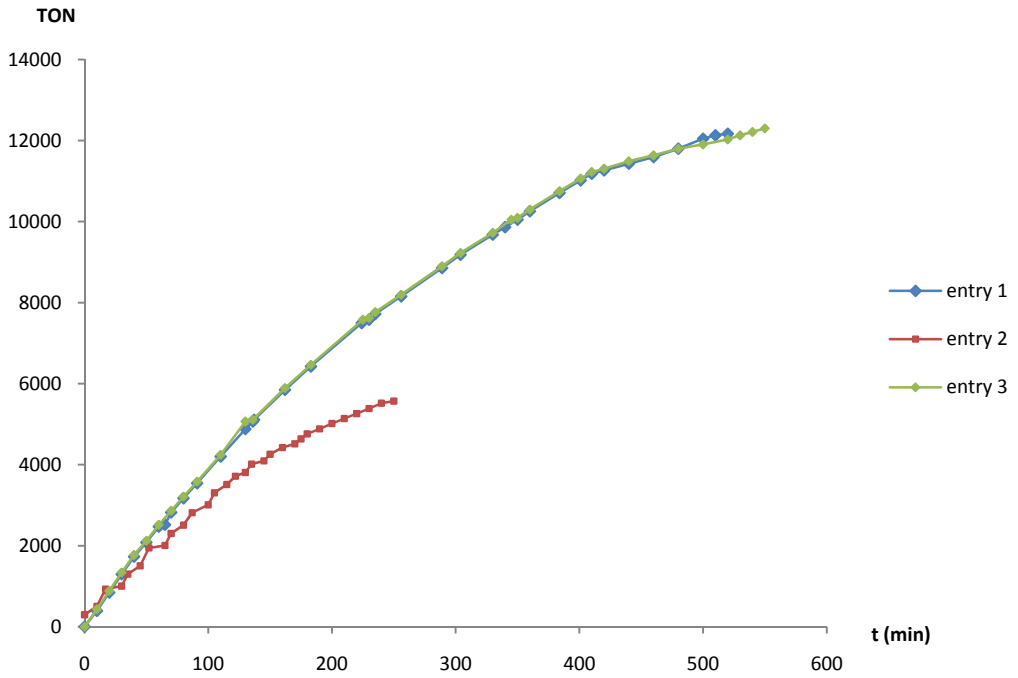

Figure S4. Reaction profiles for slow feed FA dehydrogenation with **2** and **3**. Conditions: Neat FA (12.5 mmol aliquots) added after 65, 135, 230, 350 min (entry 1); 17, 35, 52, 70, 87, 105, 122, 145, 175, 210, 250 min (entry 2); 60, 130, 225, 345 min (entry 3).

2. COMPUTATIONAL DETAILS

Calculations were performed using the GAUSSIAN 09 software package,[1] without symmetry constraints. The optimized geometries were obtained with the B3LYP functional.[2] That functional includes a mixture of Hartree-Fock[3] exchange with DFT[4] exchange-correlation, given by Becke's three parameter functional with the Lee, Yang and Parr correlation functional, which includes both local and non-local terms. The basis set used consists of the Stuttgart/Dresden ECP (SDD) basis set[5] to describe the electrons of the iron atom, and a standard 6-31g(d,p) basis set[6] for all other atoms. Frequency calculations were performed to confirm the nature of the stationary points yielding no imaginary frequency for the the minima. ^{1}H chemical sifts were calculated at the B3LYP level of theory for the optimized structures of *trans*-[Fe(PNP^{Me}-*i*Pr)(H)(CO)(η^1-OCOH)] (**4**) and *trans*-[Fe(PNP^{Me}-*i*Pr)(H)(CO)(η^1-HCOOH)]$^+$ (**5**) using the gauge-independent atomic orbital (GIAO) method in Gaussian 09 with the above basis sets. Chemical shifts are given with respect to $Si(Me_3)_4$ (TMS) at the same computational level.[7]

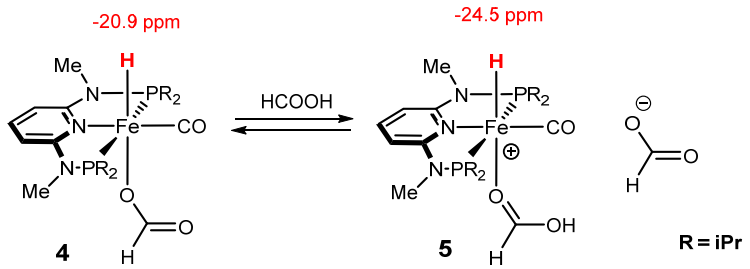

Scheme S1. Calculated ^{1}H NMR hydride shifts for *trans*-[Fe(PNP^{Me}-*i*Pr)(H)(CO)(η^1-OCOH)] (**4**) and *trans*-[Fe(PNP^{Me}-*i*Pr)(H)(CO)(η^1-HCOOH)]$^+$ (**5**).

Atomic coordinates

trans-[Fe(PNP^{Me}-*i*Pr)(H)(CO)(η^1-OCOH)] (**4**)

26	-0.006874000	-0.467660000	0.118446000
15	-2.210393000	-0.270927000	0.197924000
15	2.215235000	-0.187877000	0.143634000
7	-0.041874000	1.573026000	0.082817000
7	-2.377999000	1.471292000	0.235813000
7	2.302602000	1.553367000	-0.045780000
6	-1.226375000	2.237750000	0.123117000
6	-1.288876000	3.639850000	0.054730000
6	-0.097776000	4.345099000	-0.040043000
6	1.119221000	3.681482000	-0.067230000
6	1.116635000	2.274929000	-0.012370000
6	-3.216772000	-0.816056000	-1.308050000
6	-4.747554000	-0.845435000	-1.165956000
6	-2.692433000	-2.160806000	-1.849865000
6	-3.201688000	-0.807331000	1.701011000
6	-3.163294000	-2.336957000	1.870080000
6	-2.718374000	-0.103400000	2.977711000
6	3.103711000	-0.949703000	-1.327500000
6	4.378752000	-0.296750000	-1.879636000
6	3.311835000	-2.458720000	-1.089787000
6	3.166040000	-0.505628000	1.750688000
6	2.702448000	-1.816275000	2.414191000
6	4.704014000	-0.450335000	1.715412000
1	-2.235289000	4.159777000	0.057826000
1	-0.118700000	5.429621000	-0.096121000
1	2.040947000	4.238051000	-0.139709000
1	-2.947694000	-0.045318000	-2.041002000
1	-5.191262000	-1.120028000	-2.129614000
1	-5.177085000	0.117840000	-0.879666000
1	-5.076135000	-1.594496000	-0.438097000
1	-3.220916000	-2.405297000	-2.778449000
1	-2.867653000	-2.984715000	-1.150167000
1	-1.625037000	-2.100647000	-2.067809000
1	-4.244181000	-0.516538000	1.518401000
1	-3.774275000	-2.624062000	2.733172000
1	-2.145493000	-2.693205000	2.049140000
1	-3.556678000	-2.867483000	0.998851000
1	-3.336280000	-0.418036000	3.826616000
1	-2.782701000	0.985463000	2.899298000
1	-1.677655000	-0.360115000	3.192637000
1	2.315366000	-0.846229000	-2.082686000
1	4.702571000	-0.863198000	-2.760337000
1	5.211354000	-0.302972000	-1.168280000
1	4.202606000	0.728162000	-2.212532000
1	3.601673000	-2.927572000	-2.036373000
1	2.402786000	-2.959514000	-0.748164000
1	4.109859000	-2.662820000	-0.367971000
1	2.800958000	0.321545000	2.374446000
1	3.167813000	-1.905737000	3.402692000
1	2.996090000	-2.695758000	1.833673000
1	1.619728000	-1.835305000	2.543653000
1	5.091081000	-0.596968000	2.730644000
1	5.097544000	0.503018000	1.358008000
1	5.124347000	-1.245631000	1.093587000
1	-0.000904000	-0.379224000	1.635835000
6	0.020091000	-2.208455000	0.323813000

8	0.037472000	-3.352070000	0.530918000
6	3.549738000	2.318311000	-0.095755000
1	3.668952000	2.949781000	0.794069000
1	4.393026000	1.638842000	-0.150263000
1	3.582296000	2.956964000	-0.985531000
6	-3.659951000	2.161584000	0.358463000
1	-3.938700000	2.676911000	-0.569411000
1	-4.439349000	1.440518000	0.595047000
1	-3.632482000	2.896404000	1.170974000
8	0.118353000	-0.521569000	-1.937601000
6	-0.052722000	0.418675000	-2.812792000
8	0.512539000	0.508727000	-3.896862000
1	-0.800926000	1.200885000	-2.525457000

trans-[Fe(PNP^{Me}-*i*Pr)(H)(CO)(η^1-HCOOH)]$^+$ (**5**)

26	0.054929000	-0.511116000	-0.003161000
15	2.272352000	-0.321273000	-0.187763000
15	-2.171597000	-0.299731000	-0.220593000
7	0.063746000	1.489437000	-0.334507000
7	2.404271000	1.394956000	-0.507797000
7	-2.289573000	1.450788000	-0.275617000
6	1.243904000	2.152704000	-0.507473000
6	1.282284000	3.547395000	-0.675396000
6	0.080271000	4.239705000	-0.709618000
6	-1.130493000	3.571897000	-0.584623000
6	-1.111150000	2.178634000	-0.401182000
6	3.344302000	-0.593449000	1.349106000
6	4.868979000	-0.614493000	1.142196000
6	2.889746000	-1.846720000	2.124122000
6	3.189272000	-1.107196000	-1.620163000
6	3.156570000	-2.643940000	-1.526767000
6	2.652799000	-0.625273000	-2.976745000
6	-3.178870000	-0.863414000	1.273030000
6	-4.503369000	-0.158096000	1.609654000
6	-3.370484000	-2.393936000	1.235168000
6	-2.963313000	-0.891499000	-1.829299000
6	-2.461758000	-2.297015000	-2.216013000
6	-4.497270000	-0.827810000	-1.946511000
1	2.220089000	4.072832000	-0.777069000
1	0.085791000	5.317186000	-0.843450000
1	-2.059533000	4.118648000	-0.634725000
1	3.094092000	0.285515000	1.959473000
1	5.360865000	-0.716899000	2.115233000
1	5.256873000	0.297036000	0.682408000
1	5.184407000	-1.467141000	0.533423000
1	3.453709000	-1.917120000	3.060092000
1	3.080266000	-2.766020000	1.562878000
1	1.827458000	-1.814834000	2.372172000
1	4.234132000	-0.788468000	-1.525707000
1	3.737866000	-3.066045000	-2.352706000
1	2.137120000	-3.028627000	-1.610028000
1	3.589160000	-3.023477000	-0.597440000
1	3.261757000	-1.055561000	-3.778562000
1	2.687154000	0.462765000	-3.078008000
1	1.618189000	-0.944487000	-3.127305000
1	-2.475790000	-0.649045000	2.086481000
1	-4.910314000	-0.601069000	2.525336000
1	-5.259826000	-0.283965000	0.829973000

1	-4.372176000	0.909134000	1.801809000
1	-3.732144000	-2.729469000	2.212366000
1	-2.445156000	-2.935786000	1.028203000
1	-4.116369000	-2.693072000	0.493803000
1	-2.527709000	-0.180319000	-2.544402000
1	-2.834147000	-2.542309000	-3.215917000
1	-2.828316000	-3.068462000	-1.533493000
1	-1.372628000	-2.345745000	-2.241125000
1	-4.786174000	-1.144495000	-2.954202000
1	-4.906062000	0.173077000	-1.799231000
1	-4.988602000	-1.507068000	-1.244943000
1	0.083220000	-0.736003000	-1.473164000
6	0.052261000	-2.269434000	0.156737000
8	0.053354000	-3.426185000	0.192756000
6	-3.548751000	2.182841000	-0.470002000
1	-3.593501000	2.642293000	-1.464222000
1	-4.385172000	1.501091000	-0.368538000
1	-3.665922000	2.966517000	0.285865000
6	3.668435000	2.063354000	-0.836560000
1	3.999153000	2.730848000	-0.032150000
1	4.443687000	1.318423000	-1.000378000
1	3.569792000	2.644481000	-1.758845000
8	-0.031931000	-0.094836000	2.119843000
6	0.054615000	0.919707000	2.785575000
8	-0.073624000	0.872732000	4.105724000
1	0.236104000	1.910979000	2.343589000
1	0.019773000	1.755013000	4.497466000

3. REFERENCES

[1] Gaussian 09, Revision A.02, Frisch, M. J.; Trucks, G. W.; Schlegel, H. B.; Scuseria, G. E.; Robb, M. A.; Cheeseman, J. R.; Scalmani, G.; Barone, V.; Mennucci, B.; Petersson, G. A.; Nakatsuji, H.; Caricato, M.; Li, X.; Hratchian, H. P.; Izmaylov, A. F.; Bloino, J.; Zheng, G.; Sonnenberg, J. L.; Hada, M.; Ehara, M.; Toyota, K.; Fukuda, R.; Hasegawa, J.; Ishida, M.; Nakajima, T.; Honda, Y.; Kitao, O.; Nakai, H.; Vreven, T.; Montgomery, Jr., J. A.; Peralta, J. E.; Ogliaro, F.; Bearpark, M.; Heyd, J. J.; Brothers, E.; Kudin, K. N.; Staroverov, V. N.; Kobayashi, R.; Normand, J.; Raghavachari, K.; Rendell, A.; Burant, J. C.; Iyengar, S. S.; Tomasi, J.; Cossi, M.; Rega, N.; Millam, J. M.; Klene, M.; Knox, J. E.; Cross, J. B.; Bakken, V.; Adamo, C.; Jaramillo, J.; Gomperts, R.; Stratmann, R. E.; Yazyev, O.; Austin, A. J.; Cammi, R.; Pomelli, C.; Ochterski, J. W.; Martin, R. L.; Morokuma, K.; Zakrzewski, V. G.; Voth, G. A.; Salvador, P.; Dannenberg, J. J.; Dapprich, S.; Daniels, A. D.; Farkas, Ö.; Foresman, J. B.; Ortiz, J. V.; Cioslowski, J.; Fox, D. J. Gaussian, Inc., Wallingford CT, **2009**.

[2] (a) Becke, A. D. *J. Chem. Phys.* **1993**, *98*, 5648-5652. (b) Miehlich, B.; Savin, A.; Stoll, H.; Preuss, H. *Chem. Phys. Lett.* **1989**, *157*, 200-206. (c) Lee, C.; Yang, W.; Parr, G. *Phys. Rev. B* **1988**, *37*, 785-789.

[3] Hehre, W. J.; Radom, L.; Schleyer, P. v. R.; Pople, J. A., *Ab Initio Molecular Orbital Theory*. John Wiley & Sons, New York, **1986**.

[4] Parr, R. G.; Yang, W. *Density Functional Theory of Atoms and Molecules*, Oxford University Press, New York, **1989.**

[5] (a) Haeusermann, U.; Dolg, M.; Stoll, H.; Preuss, H. *Mol. Phys.* **1993**, *78*, 1211-1224. (b) Kuechle, W.; Dolg, M.; Stoll, H.; Preuss, H. *J. Chem. Phys.* **1994**, *100*, 7535-7542. (c) Leininger, T.; Nicklass, A.; Stoll, H.; Dolg, M.; Schwerdtfeger, P. *J. Chem. Phys.* **1996**, *105*, 1052-1059.

[6] (a) Ditchfield, R.; Hehre, W. J.; Pople, J. A. *J. Chem. Phys.* **1971**, *54*, 724-728; (b) Hehre, W. J.; Ditchfield, R.; Pople, J. A. *J. Chem. Phys.* **1972**, *56*, 2257-2261; (c) Hariharan, P. C.; Pople, J. A. *Mol. Phys.* **1974**, *27*, 209-214; (d) Gordon, M. S. *Chem. Phys. Lett.* **1980**, *76*, 163-168; (e) Hariharan, P. C.; Pople, J. A. *Theor. Chim. Acta* **1973**, *28*, 213-222.